

Volume XCII, No. 1, May 2022

Proceedings of the Danish Society for Structural Science and Engineering

Published by

Danish Society for Structural Science and Engineering

Lars German Hagsten, Lars Hestbech, Mikkel Kahlen Frandsen, Christopher Grandjean-Thomsen:
*Investigation of the buckling capacity of walls subjected to axial strip loads acting on a limited
stretch along the top of the walls end.....*1-16

COPENHAGEN 2022

Reproduction without reference to source is not permitted
Copyright © 2022 "Danish Society for Structural Science and Engineering", Copenhagen
ISSN 1601-6548 (online)

Investigation of the buckling capacity of walls subjected to axial strip loads acting on a limited stretch along the top of the walls end

Lars German Hagsten¹

Lars Hestbech²

Mikkel Kahlen Frandsen²

Christopher Grandjean-Thomsen³

1. Introduction

In the design of structures where masonry or concrete shear walls contribute to stability against horizontal loads, failure of the shear walls by buckling is often a governing factor for the wall's design. For horizontal loads that are large relative to the vertical ones, the overturning moment results in a vertical reaction that may be very eccentric, leading to a short compression zone underneath, see Figure 1a. This is in practice often handled by determining the buckling capacity of the wall per unit length, which is equivalent to treating the issue of buckling of the wall as if only a strip of the wall equivalent to the length of the compression zone underneath contributes to the buckling capacity, see Figure 1b.

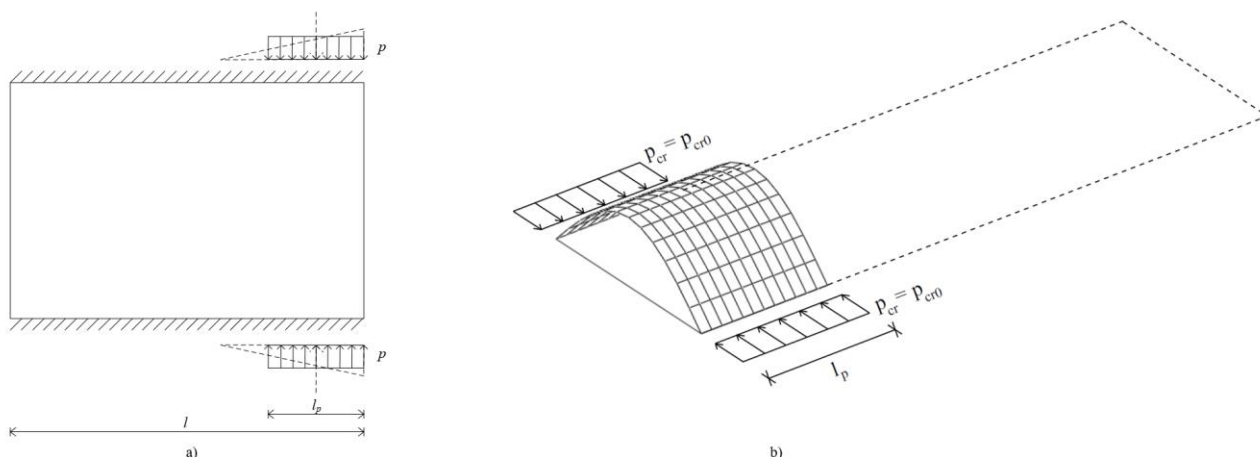


Figure 1 a): Illustration of an eccentric compression zone. b) Buckling capacity determined by considering a strip of the wall equivalent to the length of the compression zone

When the length of the compression zone is small compared to the height of the wall this is a very conservative way of estimating buckling capacity, as a larger part of the wall will be activated, see Figure 2a. This paper treats the issue by applying the energy method to determine the ratio between the actual buckling

¹ Aarhus University, Value Engineering ApS

² Søren Jensen Rådgivende Ingeniørfirma A/S

³ Value Engineering ApS

capacity of a wall subjected to a vertical load acting along the top and bottom over the length l_p , and the buckling capacity of an isolated strip of the same wall with the length of l_p . By this approach a factor k_σ is determined. The capacity of the wall can then be determined as the capacity of a strip of the wall with a length given by k_σ multiplied with the (physical) extension of the compression zone, see Figure 2b.

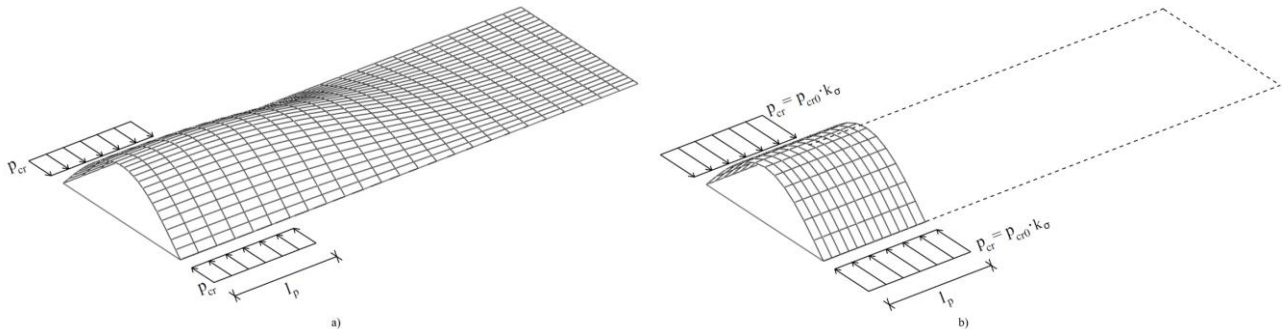


Figure 2 a): By considering the deflection of the wall it is seen that a larger part or the whole wall is activated. b) By taking the deflection of the whole wall into account this is equivalent to achieve a larger capacity over the length of the activated zone

An expression is set up to determine the load-bearing capacity of a wall supported at the top and bottom and free along the vertical sides. Both a constant distribution of the load and a linearly varying distribution of the load have been modelled. It turns out that the total result depends very little on whether one or the other modelling of the load is used.

The problem has been solved using two approaches. The first approach is having the wall affected by a triangular load, $p_{cr}(z)$, with an extension l_p , see figure 1. The load-bearing capacity is expressed as a value k_σ , multiplied with the strength of a corresponding wall affected by an evenly distributed load. In the second approach, the load is assumed to be modelled as being constant, p_{cr} , over the length l_p .

The analysis of both load scenarios is performed assuming that the wall

- is plane
- is initially without imperfections
- is with constant thickness/stiffness, see Figure 3
- is constructed of a linear elastic, isotropic and homogeneous material without residual stresses.
- is centrally loaded

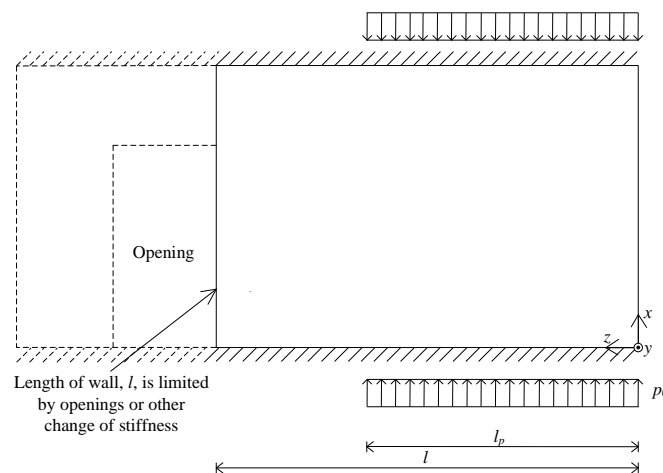


Figure 3: The length of the wall is limited by openings or other changes in stiffness. This means that holes or other openings in the wall within the length (l) are not allowed

The aim is to find the ratio, k_{σ} , between the capacities of the two load scenarios.

The expression of the load-bearing capacity is determined on the basis of energy principles. Both the inner and outer work are determined on the basis of a critical deformation figure. As the critical deformation figure turns out to vary in both directions shear deformations will also occur. The magnitude of the shear stresses due to the shear deformations are evaluated.

2. Theory

The method for determining the load-bearing capacity is initially illustrated on a wall with an evenly distributed load over the entire length of the wall as shown in Figure 4.

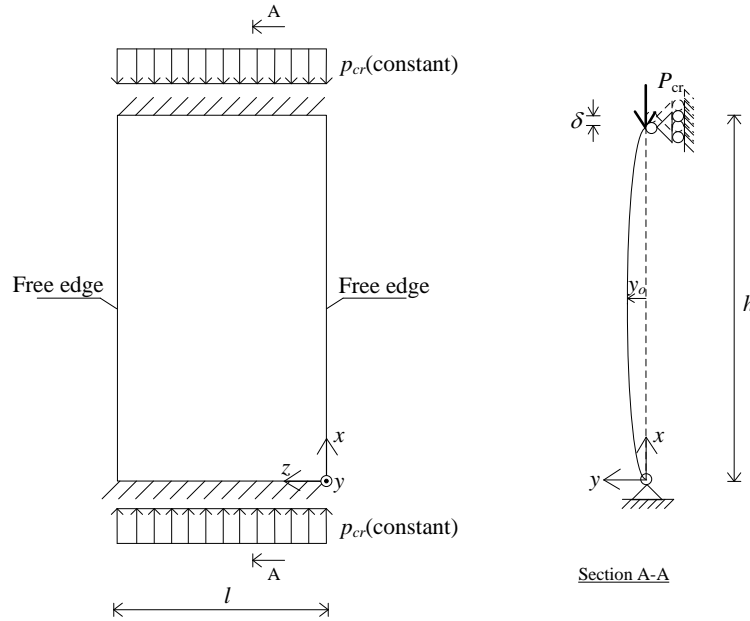


Figure 4:

The load-bearing capacity is determined by assuming a deformed state, from which the inner and outer work are set up and set equal to each other:

For a wall (a plate), the internal energy, U_i is given by [1]:

$$U_i = \frac{1}{2} D \iint_A \left(\left(\frac{\partial^2 y}{\partial x^2} + \frac{\partial^2 y}{\partial z^2} \right)^2 - 2(1-\nu) \left(\frac{\partial^2 y}{\partial x^2} \frac{\partial^2 y}{\partial z^2} - \left(\frac{\partial^2 y}{\partial x \partial z} \right)^2 \right) \right) dx dz \quad (1)$$

where

D is the flexural rigidity of the wall given by $D = \frac{E t^3}{(1-\nu^2) 12}$

The external energy for applied load in the x -direction [1]:

$$U_e = \frac{1}{2} \iint_A p_{cr}(z) \left(\frac{\partial y}{\partial x} \right)^2 dx dz \quad (2)$$

Where $\frac{1}{2} \iint_A \left(\frac{\partial y}{\partial x} \right)^2 dx dz$ expresses the vertical deflection as a function of the deformation in the y -direction. That is the shortening of the distance between the top and bottom of the wall due to the deformation of the wall.

The critical deformation figure for the wall shown in Figure 4 is:

$$y = y_0 \sin\left(\frac{x}{l} \pi\right) \quad (3)$$

where y_0 is the maximum deformation.

The magnitude of y_0 turns out to be irrelevant as it is of the same power in the inner and outer work.

By solving the equation

$$U_i = U_e \quad (4)$$

the result is found to be given by

$$P_{cr} = \frac{\pi^2 D}{h^2} \quad (5)$$

Triangular load

The capacity of the wall affected as illustrated in Figure 5 is then given by k_σ multiplied with the capacity of simply supported column/wall given in the codes.

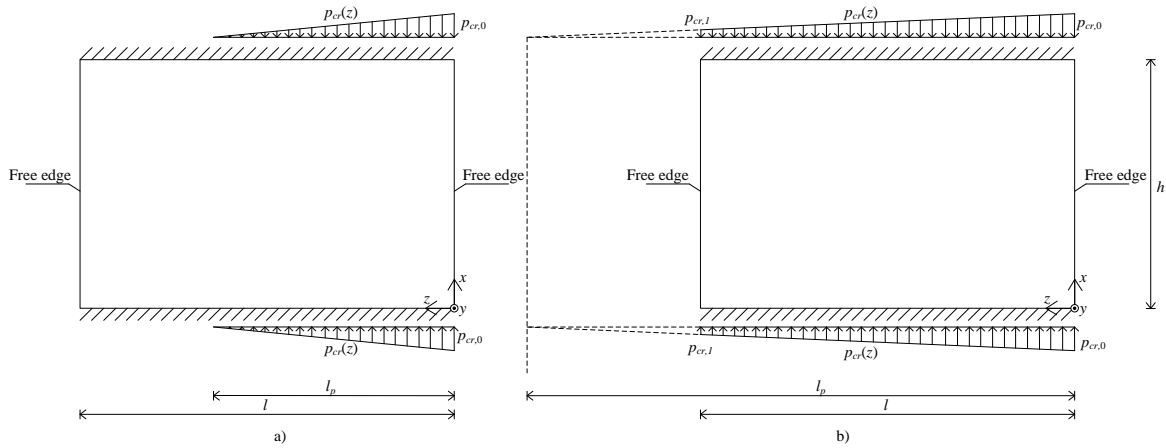


Figure 5: Wall with free vertical edges applied with linearly varying normal forces at top face. a) normal forces only at a part of the top face ($l_p < l$). b) normal forces over the whole length of the top face ($l_p > l$)

The triangular load shown in Figure 1 can be described by:

$$p_{cr}(z) = p_{cr,0} \left(1 - \frac{z}{l_p}\right) \quad (6)$$

For normal forces over the entire length of the top face ($l_p > l$), l_p is found as $l_p = \frac{p_{cr,0}}{p_{cr,0} - p_{cr,1}} l$.

Applying the presented concept of equalizing the internal and external energy, the challenge is to determine a critical deformation figure that provides minimal internal work while maximizing external work. The least possible internal work is obtained by reducing the strain energy as much as possible, and at the same time maximizing the external work which is achieved by the greatest possible movement in the direction of the load at the position where the load acts.

We consider a critical deflection form. If we look at the wall in Figure 3, both criteria can best be met by a deflection as shown in Figure 6. The deflection in the x -direction can be described by a single sin-curve and the variation in the z -direction must be limited. A linear function with $\eta < 1$ is used. For relatively longer walls (larger values of l/h) the internal energy can be reduced by also having a curvature in the z -direction as this will reduce the contribution of internal energy caused by a reduced curvature in the x -direction. By having $\eta < 1$ at the end with the smallest load the contribution to the internal energy from the curvature in the x -direction is reduced more than the contribution of the external energy and is thus more critical. The largest vertical displacements in the direction of the load are found where the load is largest (at $p_{cr,0}$).

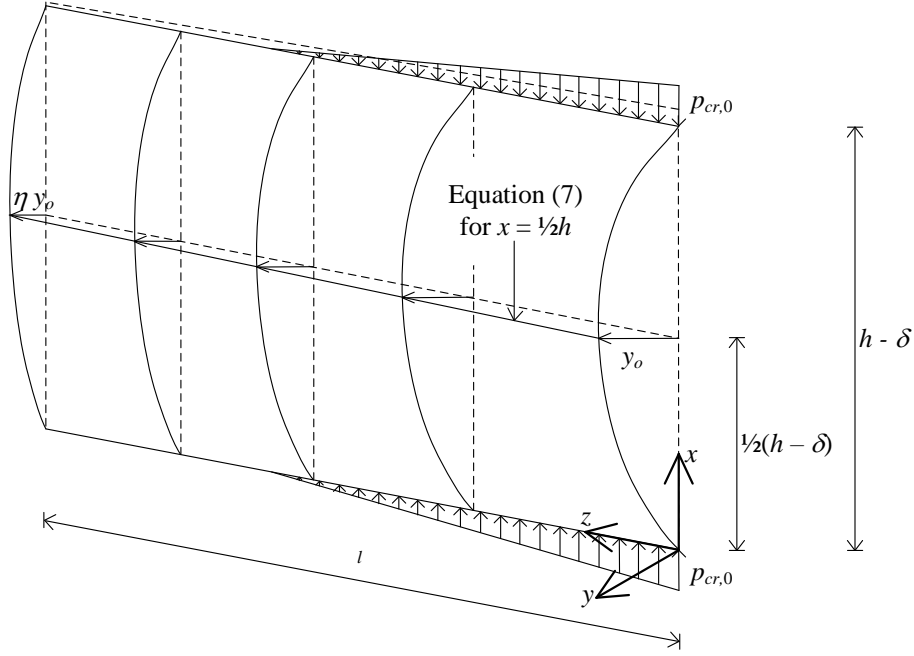


Figure 6: Illustration of the deflection. Shown for $l_p < l$. Same principal for $l_p > l$

This deflection form fulfilling these guidelines can be written with the formula:

$$y(x, z) = \left(\left(1 + (\eta - 1) \frac{z}{l} \right) + A \cdot \sin \left(\frac{2z}{l} \pi \right) \right) \cdot \sin \left(\frac{x}{h} \pi \right) \cdot y_0 \quad (7)$$

Since the displacement cannot become negative, there is a limit of A:

$$A \leq \frac{1-\eta}{2\pi} \quad (8)$$

(7) is inserted into (1) and (2).

Internal energy:

$$U_i = \frac{\pi^2 D}{h^2} \cdot \frac{1}{4} h l y_0^2 \left(\frac{\pi}{h} \right)^2 \left(\left(\eta + \frac{1}{3} (\eta - 1)^2 - 2(\eta - 1) \frac{A}{2\pi} + A^2 \cdot \frac{1}{2} \right) + 8 \left(\frac{h}{l} \right)^2 \left(-(\eta - 1) \frac{A}{2\pi} + A^2 \frac{1}{2} \right) + 16 \left(\frac{h}{l} \right)^4 A^2 \cdot \frac{1}{2} + 2(1 - \nu) \left(\frac{h}{\pi} \right)^2 \left((\eta - 1) \left(\frac{A}{2\pi} 4 \left(\frac{\pi}{l} \right)^2 \right) + (\eta - 1) \frac{1}{l^2} \right) \right) \quad (9)$$

The expression for the external energy must be divided into two expressions for $l_p \leq l$ respectively $l_p > l$.

For $l_p \leq l$:

$$U_e = p_{cr,0} \cdot \frac{1}{4} h l y_0^2 \left(\frac{\pi}{h} \right)^2 \left(\frac{1}{2} \frac{l_p}{l} + \frac{1}{3} (\eta - 1) \left(\frac{l_p}{l} \right)^2 + \frac{1}{12} (\eta - 1)^2 \left(\frac{l_p}{l} \right)^3 + \frac{A}{\pi} \left(1 - \cos \left(\frac{2l_p}{l} \pi \right) \right) + \frac{A}{\pi} \left((\eta - 1) - \frac{l}{l_p} \right) \left(\sin \left(\frac{2l_p}{l} \pi \right) \frac{1}{2\pi} - \cos \left(\frac{2l_p}{l} \pi \right) \frac{l_p}{l} \right) + \frac{A^2}{32\pi^2 l_p} \left(\cos \left(\frac{4l_p}{l} \pi \right) + 1 \right) - (\eta - 1) \frac{A}{\pi^2} \cdot \left(\sin \left(\frac{2l_p}{l} \pi \right) + \frac{1}{2\pi} \left(\frac{1}{2\pi^2 l_p} - \frac{l_p}{l} \right) \left(\cos \left(\frac{2l_p}{l} \pi \right) - 1 \right) \right) \right) \quad (10)$$

For $l_p > l$:

$$U_e = p_{cr,0} \cdot \frac{1}{4} h l y_0^2 \left(\frac{\pi}{h} \right)^2 \left(\eta + (\eta - 1)^2 \left(\frac{1}{3} - \frac{1}{4} \frac{l}{l_p} \right) - 2(\eta - 1) A \frac{1}{2\pi} + A^2 \frac{1}{2} - \left(\frac{2}{3} \eta - \frac{1}{6} - 2\eta A \frac{1}{2\pi} + A^2 \frac{1}{4} \right) \frac{l}{l_p} \right) \quad (11)$$

The capacity is found by solving (4):

By comparing with the expression for the wall affected by an evenly distributed load, the results can be put in the form:

$$p_{cr,0} = k_{\sigma} \cdot \frac{\pi^2 D}{h^2} \quad (12)$$

The expressions must be minimized with respect to η and A. The result of this optimization is shown in Figures 5 and 6, where η and A are plotted as function of l_p/l for different values of h/l . Figure 7-11 is sketched under the assumption of $\nu = 0.2$.

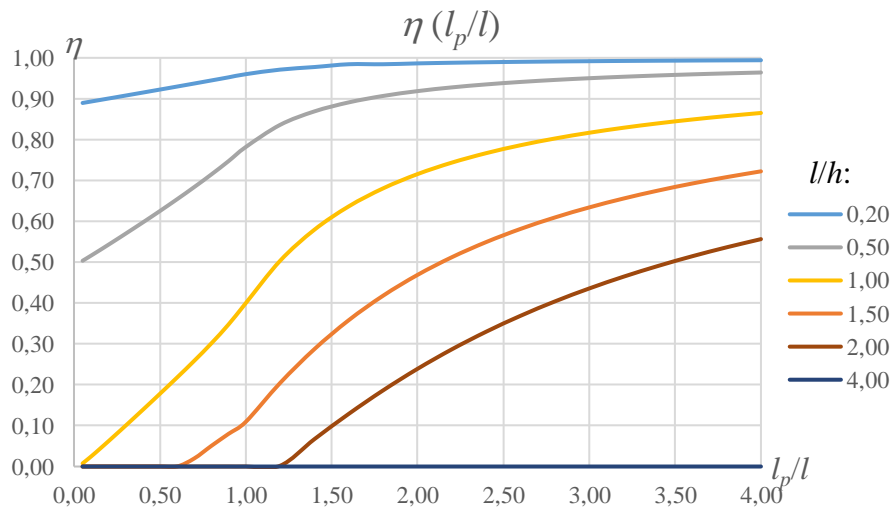


Figure 7: η as function of l_p/l for different values of h/l . Variable load

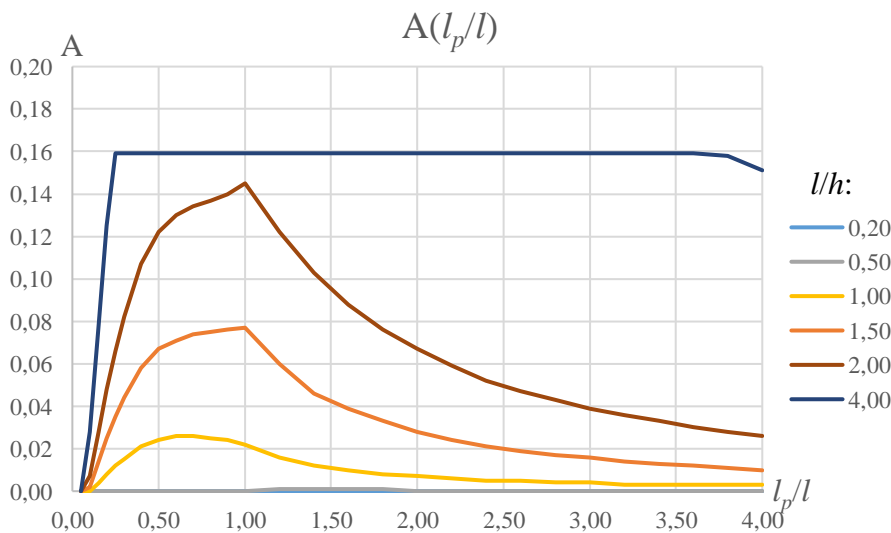


Figure 8: A as function of l_p/l for different values of h/l . Variable load

The optimization leads to the relative deflection at $x = \frac{1}{2}h$ shown in Figure 8. The axis in Figure 8 faces the opposite direction to match the deflection shape in figure 6.

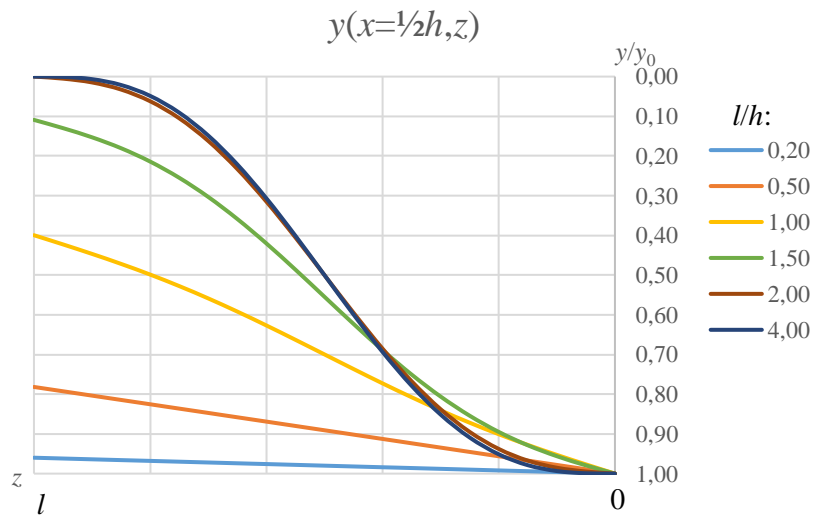


Figure 9: y/y_0 as function of l_p/l for different values of h/l . Variable load

With knowledge of η corresponding curves for k_σ can be calculated and plotted as a function of l_p/l for different values of h/l , see figure 10 and 11.

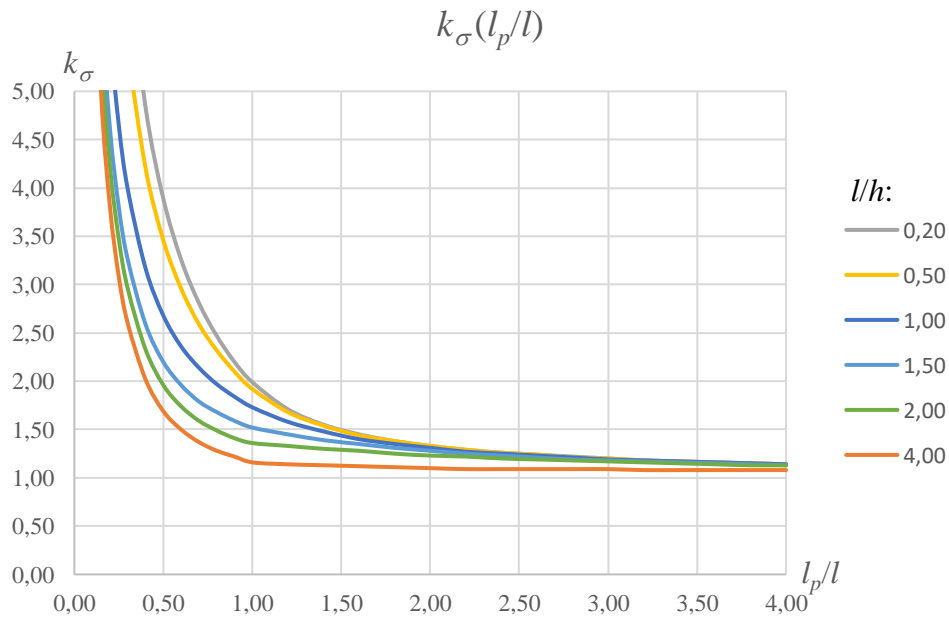


Figure 10: k_σ as function of l_p/l for different values of l/h . Shown for $l_p/l \in [0.00; 4.00]$. Variable load

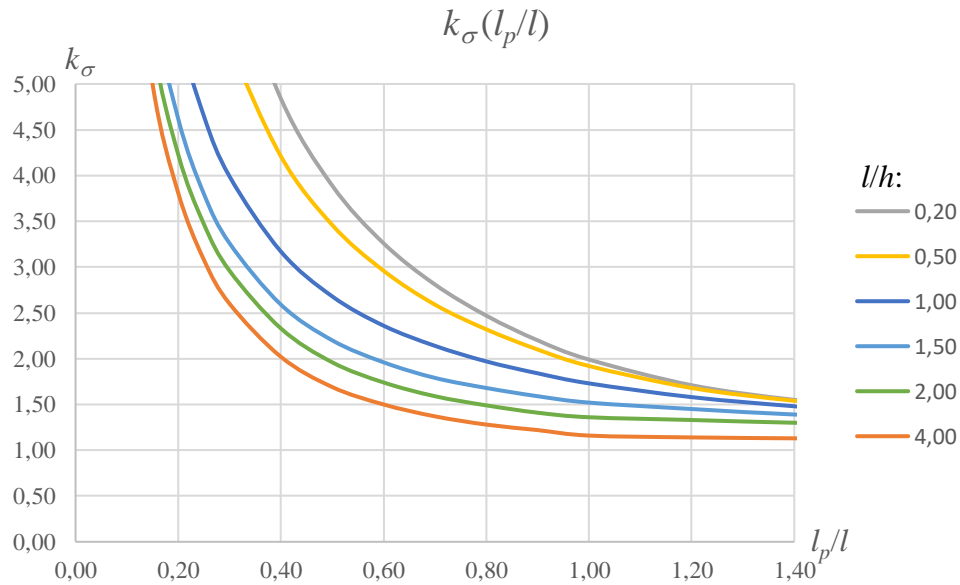


Figure 11: k_σ as function of l_p/l for different values of l/h . Shown for $l_p/l \in [0.00; 1.40]$. Variable load

An evaluation of whether the shear stresses in connection with the twisting of the wall can be carried is attached in appendix A. For concrete walls it is found that these shear stresses are not critical. For masonry walls an investigation as outlined in appendix A must be performed.

Example 1

h	6000 mm
l	3000 mm
l_p	2500 mm
t	180 mm
f_{ck}	25 MPa
f_{cd}	17.2 MPa
f_{yd}	458 MPa
ν	0.2
E_c	31000 MPa

From optimization of (4) or from Figure 6 is for $l/h = 0.5$ and $l_p/l = 0.83$ found $\eta = 0.725$ and $A = 0.002$. Inserted in (9) and (10) or read from Figure 8 is found $k_\sigma = 2.24$. To ensure that the capacity is sufficient the following inequality must be met:

$$p_{cr,0} \leq \min \left\{ \begin{array}{l} k_\sigma \cdot \sigma_{cr(code)} \\ f_{cd} \end{array} \right.$$

$\sigma_{cr(code)}$ is found to be equal to 7.29 MPa. That value is the maximum allowable normal stress at the top of the wall if the approach presented in this article is *not* applied.

$$p_{cr,0} \leq \min \left\{ \begin{array}{l} 2.24 \cdot 7.29 = 16.3 \\ 17.2 \end{array} \right.$$

The maximum normal stress at the top of the wall must not exceed $p_{rc,0} = 16.3$ MPa in order to avoid instability.

The total capacity of the wall is:

$$P_{cap} = \frac{1}{2} \cdot p_{cr,0} \cdot l_p \cdot t = 3.67 \text{ MN}$$

Constant load

If instead the load is modelled as a constant load with the intensity p_0 as shown in Figure 12, only the external load needs to be modified as the deflection is of the same form.

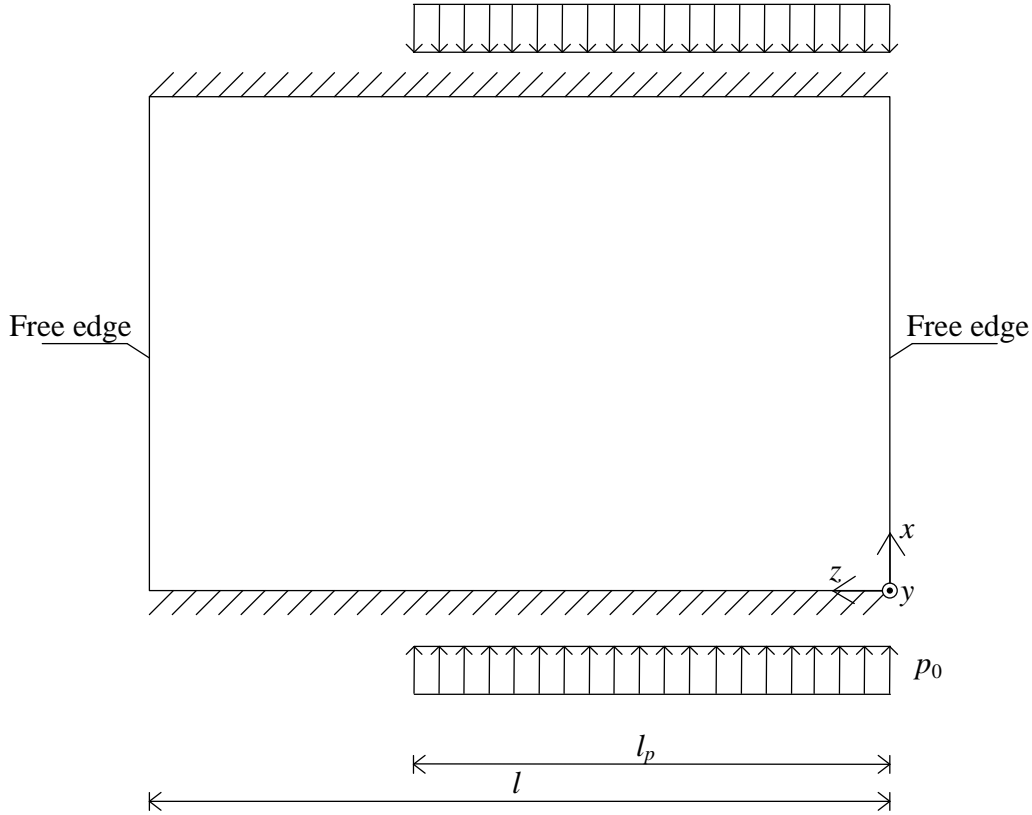


Figure 12: Wall subjected by a constant load, p_0

The external work can be expressed as:

$$U_e = \frac{1}{4} h p_{cr,0} y_0^2 \left(\frac{\pi}{h} \right)^2 \left(l_p + (\eta - 1) \frac{l_p^2}{l} + \frac{1}{3} (\eta - 1)^2 \frac{l_p^3}{l^2} + 2A \cdot \frac{l}{2\pi} \left(1 - \cos \left(\frac{2l_p}{l} \pi \right) \right) + 2(\eta - 1)A \cdot \frac{1}{l} \left(\frac{l^2 \cdot \sin \left(\frac{2l_p}{l} \pi \right)}{4\pi^2} - \frac{l \cdot l_p \cos \left(\frac{2l_p}{l} \pi \right)}{2\pi} \right) + A^2 \cdot \left(\frac{l_p}{2} - \frac{\sin \left(\frac{4l_p}{l} \pi \right) \cdot l}{8\pi} \right) \right) \quad (13)$$

Corresponding curves in the case of constant load for η , A and k_s are shown in Figures 13 - 15.

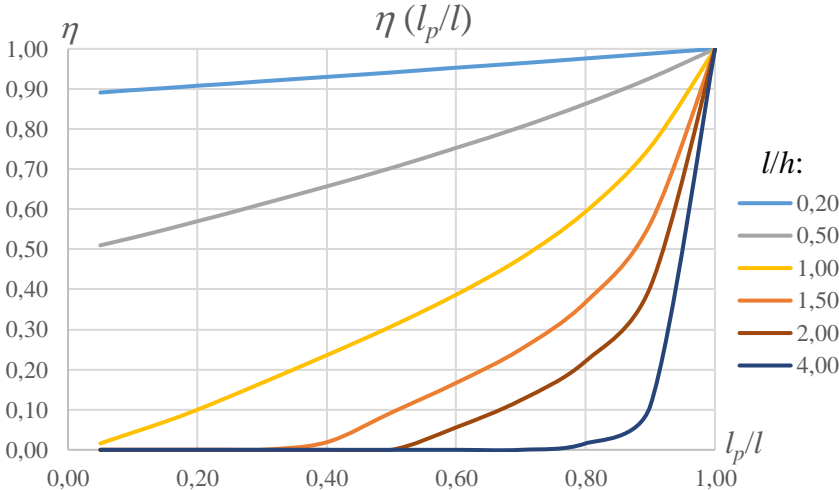


Figure 13: η as function of l_p/l for different values of h/l . Constant load

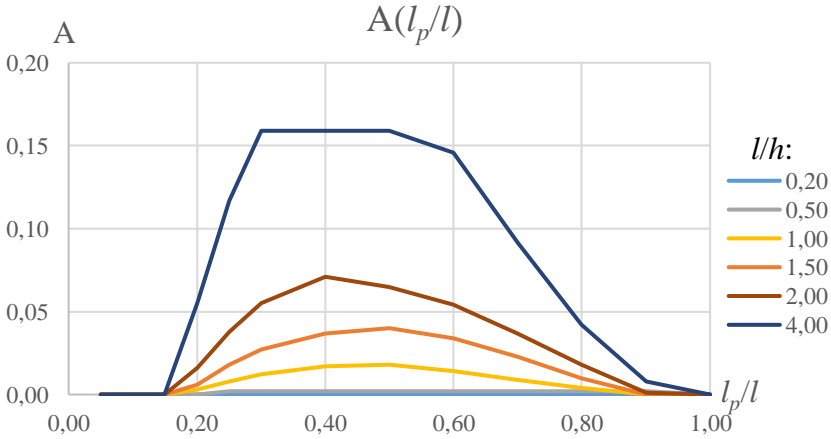


Figure 14: A as function of l_p/l for different values of l/h . Constant load

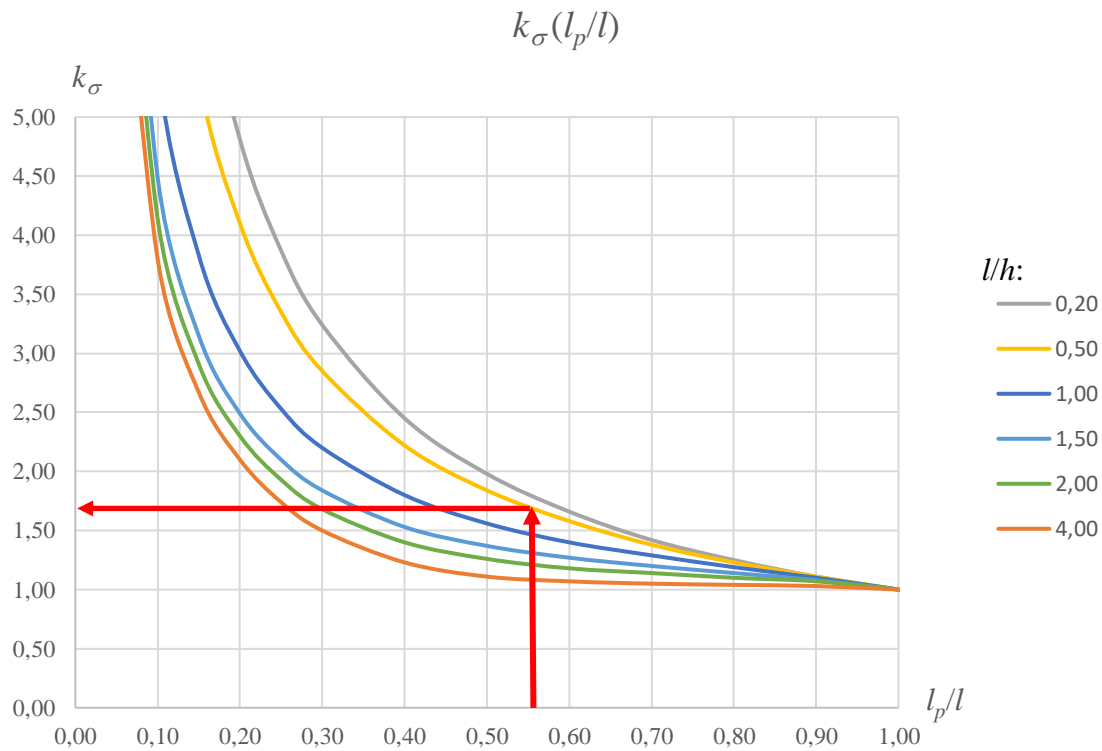


Figure 15: k_σ as function of l_p/l for different values of l/h . Constant load

Example 2

A wall with the same geometry and material as in example 1 is considered. In order to be able to compare the capacity the resultant is placed at the same distance as in example 1. That means that $l_p = \frac{2}{3} \cdot 2500 = 1667$ mm in this example.

By using $\frac{l_p}{l} = \frac{1667}{3000} = 0.556$ which we have from Figures 13 - 15 $\eta = 0.730$, $A = 0,002$ and $k_\sigma = 1.68$, it is noticed that the difference for η and A is very small compared with example 1.

The capacity is:

$$p_0 \leq \min \begin{cases} 1.68 \cdot 7.29 = 12.2 \\ 17.2 \end{cases}$$

An alternative illustration of the results presented in Figure 15 is shown in Figure 16.

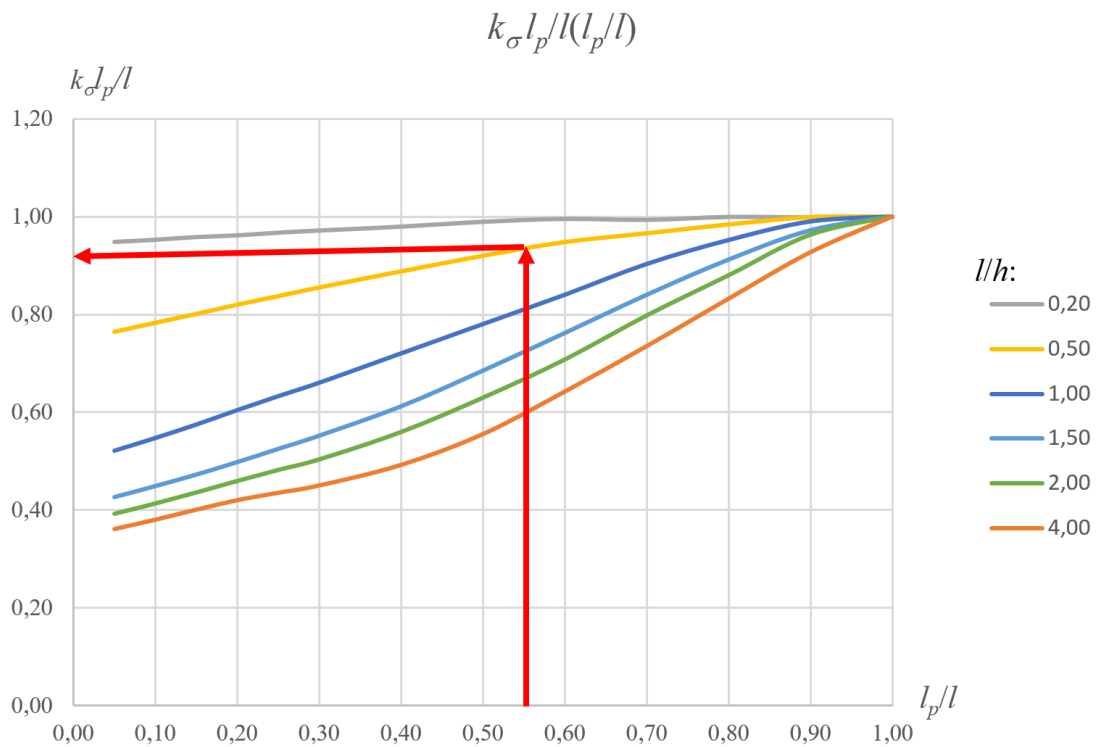


Figure 16: $k_{\sigma} l_p / l$ as function of l_p / l for different values of h / l . Constant load. The figure is in principle the same as Figure 15

In Figure 16 example 2 is illustrated. Starting at $l_p / l = 0.556$, going to the curve for $l/h = 3000/6000 = 0.50$ the value of $k_{\sigma} l_p / l$ is found as 0.93. $k_{\sigma} l_p / l = 0.93$ means that $k_{\sigma} l_p = 0.93 \cdot l = 0.93 \cdot 3000 = 2800$ mm.

Hereby the wall can be analysed using a model where the wall is simply supported at top and bottom, having a length of 2800 mm.

Due to the similarity of η and A the requirement to the shear capacity is the same.

The total capacity of the wall is:

$$P_{cap} = p_0 \cdot l_p \cdot t = 3.67 \text{ MN}$$

It is seen that the capacity is identical with the capacity found in example 1.

In Appendix B k_{σ} is shown for a wall restricted from out of plan deformations at the end opposite of the load.

3. Concluding remarks

A method for determining the buckling capacity of a wall subjected to a strip load acting at one end is presented. The method is based on energy principles and a possible form of deflection.

The commonly used method is to only take the part of the wall which is directly beneath the load into account. This investigation shows that this is a very conservative approach as most or all of the wall will be activated. The simplest way to apply the method is to look at a section of the wall which has a length corresponding to the part that is directly affected multiplied by the increase factor, k_{σ} , determined in the article.

Literature

- [1] Timoshenko, S. P., J. M. Gere. Theory of Elastic Stability. Chapter 8 and 9. Second edition. Dover Publications, Inc.
- [2] Nielsen, M. P. and Hoang, L. C. Limit Analysis and Concrete Plasticity. CRC Press, 3rd edition. 2010.
- [3] Eurocode 2 . Design of concrete structures - Part 1-1: General rules and rules for buildings. European Committee for Standardization Eurocode 2

Appendix A Evaluation of the shear stress

In order to take a larger part of the wall than l_p into account, the variation of deflection as a function of both x and z , means that shear deflection has taken place. The magnitude of the shear stresses introduced by these shear deflections need to be examined, to determine whether they are of a magnitude that exceeds the capacity of the wall. This investigation is necessary as it is an underlying assumption that the wall has the capacity to buckle in the shape described by our function $y(x,z)$. An expression for the shear stresses is determined and applied to concrete walls with h/l ratios that are commonly used in practice.

The shear stress due to the deformed deflection shape is:

$$\tau_{xz}(x, z) = 2G \cdot z \frac{\partial^2 y(x, z)}{\partial x \partial z} \quad (\text{A1})$$

The equation for $\frac{\partial y^2(x, z)}{\partial x \partial z}$ inserted gives

$$\tau_{xz}(x, z) = G \cdot t \frac{\pi}{h} \left(\left((\eta - 1) \frac{1}{l} \right) + 2 \frac{\pi}{l} A \cdot \cos \left(\frac{2z}{l} \pi \right) \right) \cos \left(\frac{x}{h} \pi \right) \cdot y_0$$

The extreme values of $\tau_{xz}(x, z)$ are found at the top and bottom ($x = \begin{cases} 0 \\ h \end{cases}$) at $z = 1/2l$:

$$|\tau_{xz}| = \frac{\pi t y_0 G}{lh} (1 - \eta + 2\pi A) \quad (\text{A2})$$

The problem is that the magnitude of stresses is a function of the magnitude of the deflection. In the used analysis for calculating the capacity, the magnitude of the deflection remains unknown as y_0 is of the same order in the internal and external work and therefore so far has played no part.

In order to evaluate the influence of the shear an estimation of y_0 is made

$$y_0 \sim \frac{1}{10} \frac{1}{r} \cdot h^2 \quad (\text{A3})$$

where $\frac{1}{r}$ is found based on the stress distribution at the section with the largest normal stress, σ_{cr} , shown in Figure A9a. Estimation of the curvature is based on the assumption that the normal stress at the most compressed edge of the critical load is equal to f_{cd} .

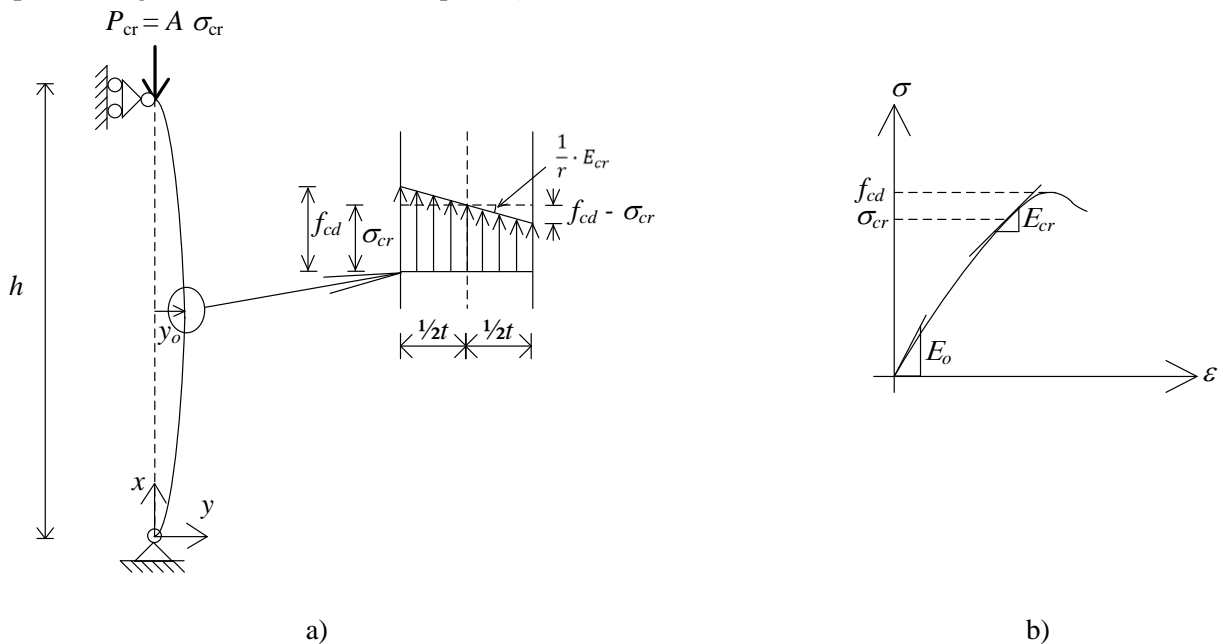


Figure A1: a) Stress distribution. b) Illustration of the variation of E

Under this assumption the curvature is expressed as:

$$\frac{1}{r} = \frac{f_{cd} - \sigma_{cr}}{1/2t} \cdot \frac{1}{E_{cr}} \quad (A4)$$

Various numerical simulations based on a stress-strain relation according to EC2, formula (3.14) and a imperfection equal to $h/400$ have shown that this is a conservative estimate of the curvature. In these numerical simulations the tasks are to equalize the eccentricity of the force in the column with the sum of the imperfection and the deflection. In these numerical studies σ_{cr} is determined by $\frac{f_{cd}}{1 + \frac{f_{cd}}{\pi^2 \cdot E_{ocr}} \lambda^2}$.

The stress-strain relation is sketched in Figure A9b. According to Ritter Young's modulus can be expressed as:

$$E_{cr} = \frac{f_{cd} - \sigma_{cr}}{f_{cd}} \cdot E_o \quad (A5)$$

Inserted in the expression for the curvature:

$$\begin{aligned} \frac{1}{r} &= \frac{f_{cd} - \sigma_{cr}}{1/2t} \cdot \frac{f_{cd}}{f_{cd} - \sigma_{cr}} \cdot \frac{1}{E_o} \\ \frac{1}{r} &= \frac{2f_{cd}}{t \cdot E_o} \end{aligned} \quad (A6)$$

(A6) inserted into (A3) lead to:

$$y_0 \sim \frac{1}{5} \cdot \frac{f_{cd}}{E_o} \cdot \frac{h^2}{t} \quad (A7)$$

(A7) inserted into (A2) lead to:

$$|\tau_{xz}(y = 1/2t)| \sim \frac{\pi(1-\eta+2\pi A)}{10(1+\nu)} \frac{h}{l} f_{cd} \quad (A8)$$

In concrete the shear capacity can be found by:

$$\tau_R = c + \mu\sigma \quad (A9)$$

In vertical sections no normal stresses will be present, meaning that $\tau_R = c$. According to [MPN] $c = \frac{f_{cd}}{k}$,

$k = \frac{1+\sin\varphi}{1-\sin\varphi} = 4$, the following inequality must be fulfilled:

$$\frac{\pi(1-\eta+2\pi A)}{10(1+\nu)} \frac{h}{l} f_{cd} \leq \frac{f_{cd}}{k} \quad (A10)$$

The most critical situation is found for $l/h = 0.75$ for very small values of l_p ($l_p/l = 0.05$). In this case the left side of (A10) exceeds the limit with less than 10%. Due to the conservative assessment of the maximum deflection, y_0 , this limited exceedance is considered to be acceptable.

In horizontal joints in masonry the shear capacity can be found by:

$$\tau_R = f_{vm0} + \mu_{fm}\sigma \leq f_{vmlt} \quad (A11)$$

For masonry walls it must be checked that the shear stress found by (A8) does not exceed the capacity found by (A11).

Appendix B k_σ for a wall restricted from out of plan deformations at the end opposite of the load

In figure B.1 a wall restricted from out of plan deformations is shown at the edge opposite of the load. The restriction of this deformation could be caused by a transverse wall.

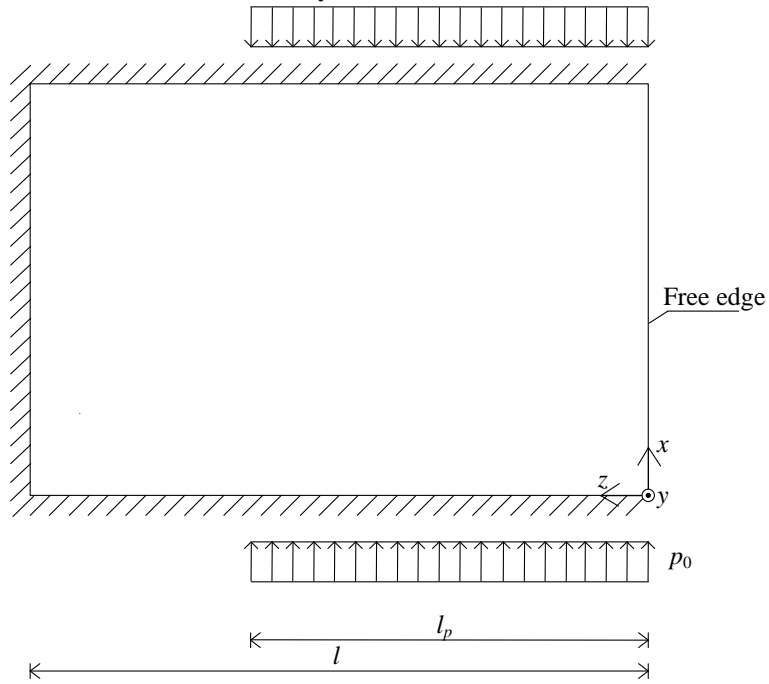


Figure B.1: Wall restricted from out of plan deformations at the end opposite of the load ($\eta = 0$)

In figure B.2 k_σ for a wall restricted from out of plan deformations at the end opposite of the load is shown. The figure replaces Figure 15 in the case of a restriction at the supported end. The largest deviations between the graphs in Figure 15 and Figure B.2 are seen in the lowest values of l/h .

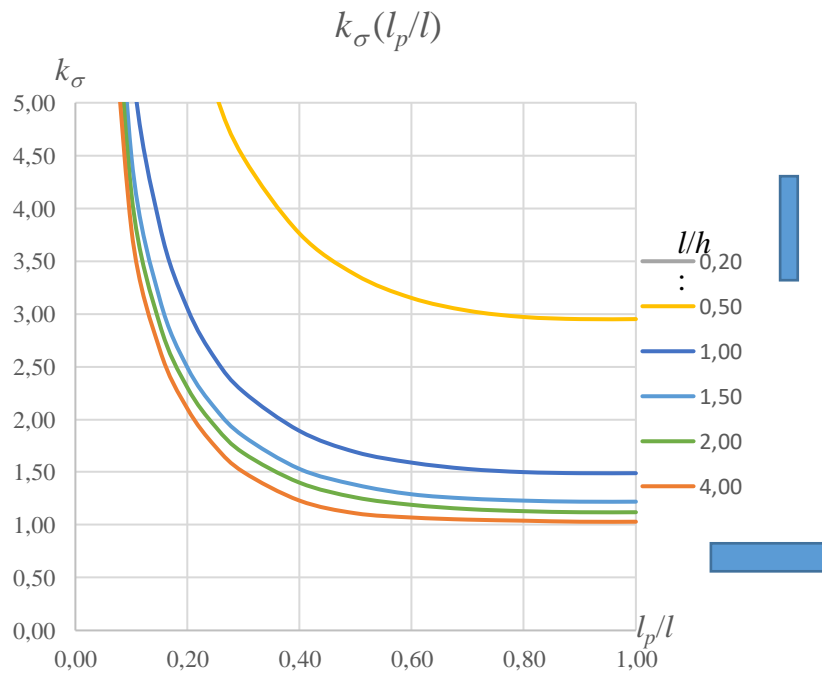


Figure B.2

Danish Society for Structural Science and Engineering

Requests for membership of the society are submitted to one of the board members:

Kåre Flindt Jørgensen, Chairman of the Board
NCC Danmark. Mail: karjor@ncc.dk

Andreas Bollerslev, Vice Chair
Niras. Mail: anbo@niras.dk

Kirsten Riis, Secretary
Vejdirektoratet. Mail: kiri@vd.dk

Mikkel Christiansen, Cashier
AB Clausen. Mail: dsby.mc@gmail.com

Gunnar Ove Bardtrum, Board member
BaneDanmark. Mail: goba@bane.dk

Jesper Pihl, Board member
Cowi. Mail: jepi@cowi.dk

Dennis Cornelius Pedersen, Board member
MOE. Mail: dcpe@moe.dk

Jens Henrik Nielsen, Board member
DTU. Mail: jhn@byg.dtu

The purpose of the society is to work for the scientific development of structural mechanics - both theory and construction of all kinds of load-bearing structures - promote interest in the subject, work for a collegial relationship between its practitioners and assert its importance to and in collaboration with other branches of engineering. The purpose is sought realized through meetings with lectures and discussions as well as through the publication of the Proceedings of the Danish Society for Structural Science and Engineering.

Individual members, companies and institutions that are particularly interested in structural mechanics or whose company falls within the field of structural mechanics can be admitted as members.